TELKOMNIKA Telecommunication, Computing, Electronics and Control
Vol. 18, No. 3, June 2020, pp. 1259~1267
ISSN: 1693-6930, accredited First Grade by Kemenristekdikti, Decree No: 21/E/KPT/2018
DOI: 10.12928/TELKOMNIKA.v18i3.12960

A hybrid algorithm for wave-front corrections applied to satellite-to-ground laser communication

Mohammed Senan Al Gobi[1], Djamel Benatia[2], Mouadh Bali[3]
[1,2]Electronic Department, Laboratoire d'Électronique Avancée (LEA), Faculty of Technology, University of Batna 2, Algeria
[3]Department Computer Science, Faculty of Exact Sciences, Université d'El Oued, Algeria
[3]LIMED Laboratory, Faculty of Exact Sciences, Université de Bejaia, Algeria

Article Info

Article history:

Received Sep 18, 2019
Revised Dec 7, 2019
Accepted Dec 21, 2019

Keywords:

Adaptive optics (AO)
Genetic algorithm
Object-oriented matlab adaptive optics (OOMAO)
Satellite-to-ground
Wave-front correction

ABSTRACT

Laser communications hold accurate data rate for ground satellite links. The laser beam is transmitted through the atmosphere. The clear-air turbulence induces a number of phase distortions that damage wave-front. Adaptive optics (AO) treats wave front correction. The nature of AO systems is iterative; it can be integrated in metaheuristic algorithms such as genetic algorithm (GA). This paper presents improved version of algorithm for wave-front corrections. The improved algorithm is based on genetic algorithm (GA) and adaptive optics approach (OA). It is implemented in a computer simulation model called object-oriented matlab adaptive optics (OOMAO). The optimisation process involves best possible GA parameters as a function of population size, iteration count, and the actuators' voltage intervals. Results show that the application of GA improves the performance of AO in wave-front corrections and the communication between satellite-to-ground laser links as well.

Corresponding Author:

Mohammed Senan Al Gobi,
Electronic Department, Laboratoire d'Électronique Avancée (LEA),
Faculty of Technology, University of Batna 2,
Batna, Zip 05000, Algeria.
Email: moh.algobi@gmail.com

1. INTRODUCTION

The communication satellite systems with optical laser links have become priority in communication fields for number of reasons. Compared to the radio communication which needs more than 1 Gbps [1, 2], the communication satellite systems with optical laser links data rate is higher (more than 10 Gbps bit rate [3]), signal intensity (structure of fiber laser [4, 5]) and lower equipment size [5]. It has made a significant contribution in reducing the effects of atmospheric attenuation that is also determined by the geographic location especially in the tropical and equatorial regions where the rain effect plays an important role in the quality of communication [6-8], as it leads to the instability in the intensity and the phase of the received signals [1, 9]. In laser satellite communications, the elements of the atmosphere (wind, rain, dust…) can affect the quality of communication [5]. The problem occurs when the optical wave propagates in free space and is subjected to serious disturbances (wave-front sensor) which renders the system less effective and probably loses the information.

In adaptive optics (AO), the most important element is the deformable mirror. Which controlled by the approximation algorithms [9]. There are many algorithms that can correct wave front sensor such as: the stochastic parallel gradient descent (SPGD), simulated annealing (SA), and genetic algorithm

(GA) [10, 11]. This contribution provides a hybrid solution to correct wave front sensor. The provided solution consists of the combination of GA with AO solution. The hybrid solution gives positive results in correcting the wave front aberration in satellite laser communication.

The present paper is divided into five sections. A brief overview of the effects of atmosphere attenuation on the refractive index's behaviour is presented in section two. In section 3 provides the design and implementation of the genetic algorithm (GA) and the hybrid (GA and AO). Section 4 is dedicated to the discussion of the obtained results. The last section is devoted to the overall results of our study and future works.

2. BACKGROUND OF THE STUDY

When the optical signal (laser here) passes through the atmosphere, it gets exposed to atmospheric attenuations i.e. clouds, rains, winds, dust. As a result, the satellite-to-ground optical links will be degraded. Figure 1 illustrates the overall frequency behavior of the real part of the index of refraction. Atmospheric attenuations is the aberration in wave-front deformation. It reduces the intensity and the phase of the received signals. As result, it decreases the image's resolution. To correct phase aberration, wave-front correction is implemented using adaptive optics (AO) technology [5, 9].

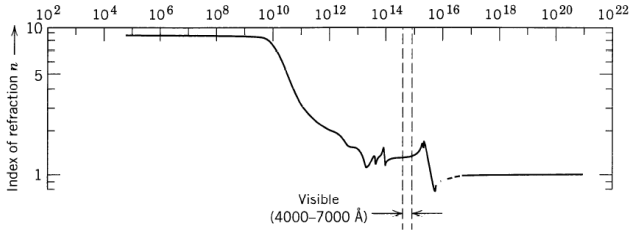

Figure 1. Behavior of the index of refraction as a function of linear frequency [12]

2.1. The theory of atmospheric fluctuations

Atmospheric fluctuation at Ka-band frequencies is commonly known as atmospheric turbulence. Each point in the telescope aperture receiving is considered as the sum of many components distributed by the turbulent eddies. Constructive interference of laser waves appear as spots of light. These spots represent the waves interfered constructively. However, destructive interference appears as dark area. The effects of atmospheric turbulence are refined by changing the telescope aperture and by reducing the amplitude scintillations observed at the receivers [13].

2.1.1. Classical atmospheric turbulence

Two extreme turbulent scales (the internal l0, and the external scale L0) have been identified to model the atmospheric turbulence [5, 8]. The internal scale l0 (r, t) corresponds to the spatial scale from which the kinetic energy is dissipated in heat by viscous friction. Therefore, it depends on the density of the atmosphere. l0 (r, t) can vary from a few millimetres near the ground to a few centimeters in the tropopause (interface between the troposphere and the stratosphere) [9]. The external scale L0 (r, t) (ranging from 10-100 meters) is determined by the size of the of air masses. It corresponds to the largest macroscopic phenomena (air layers, winds, weather disturbances). The inertial domain defines the scales for which turbulence is fully developed. It determines limiting value of the external scale of turbulence L0 and the internal scale of turbulence l0 [9]. In a turbulent air, the random variations of refractive index, n, are described by the structure function, Dn [13].

$$D_n(\rho) = \langle |n(r) - n(r+\rho)|^2 \rangle \quad (1)$$

The difference between the value n (r) at a point r and the value n (r +ρ) at a point (r +ρ) is a point distant from the vector r in a distance ρ. It represents a position in a three-dimensional space [14]. For an established turbulent regime in the inertial domain, the variance of the difference at two points of space, or structure function, is given by:

$$D_n = \begin{cases} C_n^2 \rho^{2/3}, & {}^1/_{l_0} \le \rho \le {}^1/_{L_0} \\ C_n^2 l_0^{2/3} \left(\frac{\rho}{l_0}\right)^2, & \rho < {}^1/_{l_0} \end{cases} \quad (2)$$

where C_n^2 is the structure function constant expressed in $m^{-2/3}$ and displacement ($\rho = |\rho|$) is a scalar measured by m. C_n^2 is typically vary between 10^{-13} $m^{-2/3}$ and $10^{-15} m^{-2/3}$ for strong turbulence and weak turbulence respectively [5, 15].

2.1.2. Spectral density and variance of refractive index

According to the Wiener-Khinchine theorem, the power spectral of the spatial fluctuations is calculated using simple Fourier transform [14]:

$$\emptyset_n(k) = 0.033 C_n^2 k^{-11/3} \quad (3)$$

k: is the modulus of the spatial frequency (Kolmogorov spectrum) that is expressed in m^{-1}. The Kolmogorov spectrum (3) is valid only in the inertial domain: $1/L_0 < k < l/1_0$. It represents an external scale and an internal scale of turbulence respectively [14].

The variance of intensity fluctuations $\sigma_\chi^2(dB^2)$ at the terminal point of the receiver after an (initially) plane wave with wave-number $k=2\pi/\lambda$ has propagated through a depth L of homogeneous turbulence is [13, 15]:

$$\sigma_\chi^2 = \begin{cases} 186\, l_0^{-7/3} C_n^2 L^3 \ , & l_0 > \sqrt{\lambda L} \\ 23.2\, C_n^2\, k^{7/6}\, L^{11/6} \ , & L_0 \ll \sqrt{\lambda L} < l_0 \\ 75.4\, \langle (\Delta n)^2 \rangle L L_n k^2 \ , & L_0 \ll \sqrt{\lambda L} \end{cases} \quad (4)$$

where $\langle (\Delta n)^2 \rangle$: is square refractive index fluctuation and L_n is the integral scale of the turbulence of the same order as L_0. The first expression on the right side of (4) refers to the optical regime whereas the second expression is the diffraction regime. The latter plays an important role in microwave scintillation that occurs on Earth–space paths. At the terminal point of the receiver, the expected spectral density, $W_\chi(\omega)$ of the signal is flat at a low frequency and rolls off at high frequencies. The asymptotic behaviour is given by [15, 16].

$$W_\chi(\omega) \rightarrow \begin{cases} 2.765 \frac{\sigma_\chi^2}{\omega_t} \ , & \omega \rightarrow 0 \\ 7.13 \frac{\sigma_\chi^2}{\omega_t} \left(\frac{\omega}{\omega_t}\right)^{-8/3} \ , & \omega \rightarrow \infty \end{cases} \quad (5)$$

where $\omega_t = v_t\,(k/L)^{1/2}$ is the Fresnel frequency and v_t is the component of the wind velocity transverse to the propagation path. The two asymptotes intersect at a corner frequency, ω_c, which depends on v_t. For a thick layer of uniform (homogeneous) turbulence $\omega_c = 1.43\ \omega_t$ [13].

2.2. Principal of adaptive optics

Adaptive optics (AO) technology helps correcting the phase aberration in the laser wave-front caused by atmosphere turbulence in real time. AO is used in space field and in a number of fields such as: ophthalmology [17]. Recently the adaptive optics is also used in the two-photon excitation microscopy [17]. To correct the wave-front in the optical systems, AO systems are used with a deformable mirror (DM) [10, 17]. In our study, optimization algorithms individually controls The 92 actuators' deformable mirror. They put each actuator in the right position by changing the mirror surface shape to produces a suitable wave front for the system [11].

2.2.1. Wave-front analysis

Unlike in the radio frequency field, it is not yet possible to measure the phase of the wave-front at optical wavelengths directly. Optical detector is incapable to respond to temporal frequencies. This problem is overcome by performing indirect measurements i.e. by analyzing the impact of phase disturbances on the intensity distribution [9]. Rousset carries out a description to analyzers for adaptive optics [18]. The Shack-Harmann analyser is commonly used in adaptive optics because its limitations are the representatives of those of most planar pupil analyzers [14].

2.2.2. Principal of the Shack-Hartmann analyzer

The Shack-Hartmann wave surface analyzer (SH) is a pupil plane analyzer as shown in Figure 2. It is based on the geometrical optics formalism [19]. A micro-lens array samples the incident wave-front in the pupil plane. A measurement of the position of the image spot formed at the focus of each of the micro-lenses gives access to the local slope of the wave-front in the pupil plane of each micro-lens [14]. The measurement of the position is often carried out by the center of gravity, but other positional estimators

can also be used, such as correlation [19-21]. The slope measured by the center of gravity in each sub-pupil k is respectively for the direction in x and y:

$$P_x^k = \frac{\iint dr \frac{\delta\varphi_k(r)}{\delta x} |\psi_k(r)|^2}{\iint dr |\psi_k(r)|^2} \quad (6)$$

$$P_y^k = \frac{\iint dr \frac{\delta\varphi_k(r)}{\delta y} |\psi_k(r)|^2}{\iint dr |\psi_k(r)|^2} \quad (7)$$

where the double integration is carried out on the surface of the sub-pupil k considered, φ_k the phase and $|\psi_k|$ the amplitude of the complex field. When the intensity is constant in each sub-pupil, the slope measurement is then an average on the surface of the sub-pupil.

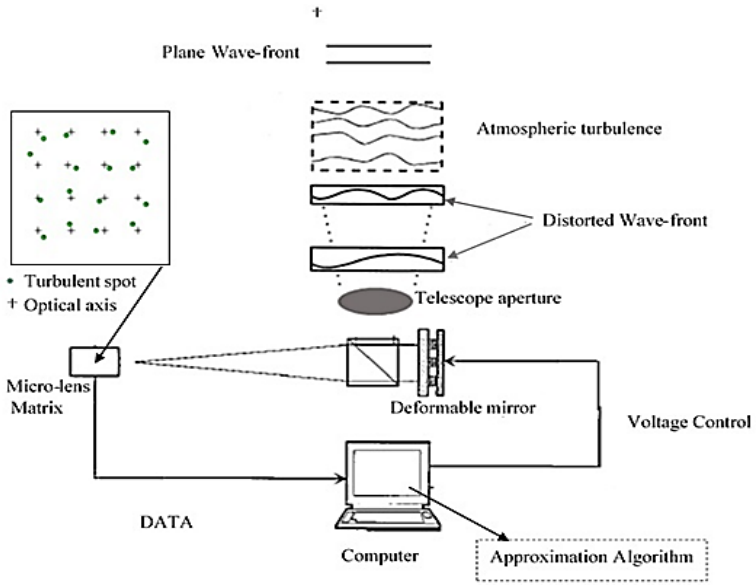

Figure 2. Schema of an adaptive optics system and the Shack-Hartmann wave-front analyser

2.3. Genetic algorithm

Genetic algorithm (GA) is a stochastic parallel algorithm that uses Darwin's theory of species evolution. It is based on three principles: variation, adaptation and inheritance [22, 23]. Variation: every individual within a population is different. The differences, more or less important, will be decisive in the process' selection. Adaptation: The most adapted individuals to their environment reach adulthood more comfortably. Individuals with better survivability will therefore be able to reproduce more. Heredity: The characteristics of individuals must be hereditary in order to be transmitted to their descendants. This mechanism will make it possible to evolve the species to share the advantageous characteristics to its survival [23-25]. In the present work, population refers to the possible collection of solutions. However, the individual represents a solution. Chromosome, in the other hand, is a component of the solution and gene represents a characteristic (or a peculiarity).

2.4. Object-oriented matlab adaptive optics (OOMAO)

Object-Oriented Matlab Adaptive Optics (OOMAO) is a library of Matlab classes, dedicated to adaptive optics (AO) systems. The main classes used in this toolbox are: source, atmosphere, telescope, Shack-Hartmann, deformable mirror [26, 27]. The source class is the link between other classes. The atmosphere class contains all the parameters defining the atmosphere. A multilayer atmosphere is created by setting the appropriate vectors of altitudes, wind speeds and directions and turbulence strengths. An atmosphere object needs to be coupled with a telescope object to create a 3-D volume of turbulence phase screens. The telescope class contain the telescope parameters and the phase screens in the turbulent layers set by an atmosphere object. In a closed-loop adaptive optics system, the deformable mirror is the first active component that encounters the wave front. To complete an Adaptive Optics System, there must be a wave front sensor. The OOMAO implements the wave front sensor [26, 28].

3. OUR PROPOSED SLOUTION

In this section, we discuss the design of a hybrid solution based on OOMAO closed-loop with the assistance of the genetic algorithm.

3.1. Genetic algorithm notation

- Population: matrix Pop(NxM) of real numbers contains the set of solutions generated by one iteration as shown in Table 1: where N is the number of solutions (or chromosomes) and M is the number of actuators in DM (or genes).
- Chromi: vector of real numbers contains the solution (i) in the population.
- Genej: real number, represents the value of the assigned voltage to the actuator j in the DM

Table 1. Population coding

I x J	Gene1	Gene2	….	$Gene_j$
Chrom1	0.08	0.0025	…	-0.036
Chrom2			…	
...			…	
…			…	
Chromi			…	

3.2. Hybrid algorithm flow-chart

The main steps of the processes in our Algorithm are:

- Initialization : values are assigned to GA parameters (population size, iterations count…), and generate the chromosomes by assigning random values to their genes.
- Evaluation : fitness function is defined to determine the adaptation score of chromosomes during the selection process. We define the fitness (i) for chromi.

$$\boldsymbol{Fitness(i)} = \frac{\sum_{j=1}^{M} \sigma_{ij}}{M} \tag{8}$$

where $\boldsymbol{\sigma}$ij is the standard deviation for Gaussian mutations of the sensor j, and M is the number of the actuators.

- Selection: according to the roulette method of selection, we select a set of best chromosomes, will be referred to as parents, in order to reproduce the next generation. The Figure 3 illustrates the main steps of the processes in hybrid algorithm solution.

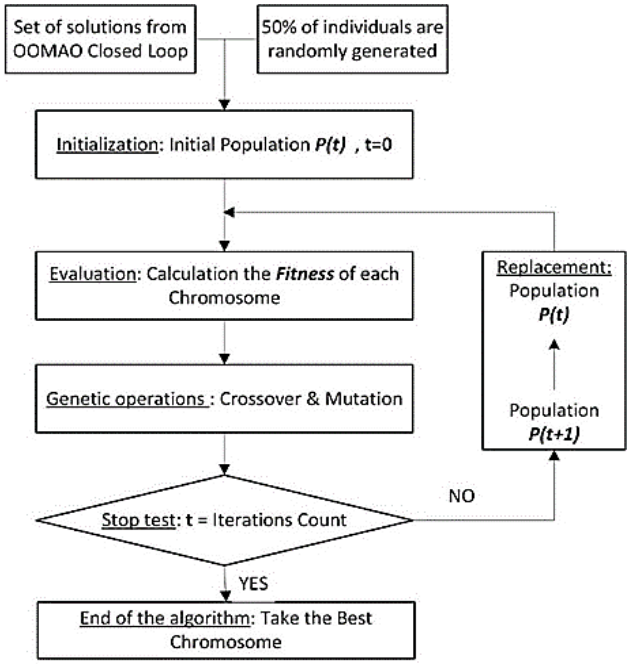

Figure 3. Flow-chart of the hybrid solution

4. RESULTS AND DISCUSSION

Our experimental work has passed into two steps. Firstly, we looked for the best configuration for genetic algorithm parameters (population size-iteration count-actuator current interval), in order to get the best performance of the genetic algorithm. The second step is the execution of the OOMAO closed loop [28] and let the genetic algorithm use the obtained results in its initial population (as 50% of individuals). Also, it uses the best parameters from the first step. Then, we made a comparison between OOMAO closed loop and our hybrid algorithm.

4.1. AO parameters

For AO parameters, data are amassed by using OOMAO founders in [26, 28]. We present them in Table 2.

Table 2. AO parameters as used in this analyse

	Parameter	Value
Atmosphere	Altitude	[0, 4000, 10000]
	fractionnalR_0	[0.7, 0.25, 0.05]
	Wind speed	[5, 10, 20]
	Wind Direction	[0, pi/4, pi]
Source	Wavelength	60
Shack Hartmann (wave sensor)	Wave front sensing	700nm
	lens let array	92
	Camera	542 pixels
	Diameter	8m
Telescope	Resolution	54
	Field of View	2.5 arc minute
	Sampling Time	500Hz

4.2. GA parameter

Using the data shown in Table 2, we made more than 60 experiments in differents situations using a number of GA paramaters such as: population size, Iterations number and Min (and Max) value of voltage. To obtain the best GA parameters, we plot the root mean square values in µm of the wave-front corrections as a function of population size, iteration accounts, and voltage intervals. Results are shown in Figures 4, 5, and 6 respectively. Table 3 summarizes the GA parameters as obtained from this study. Figure 4 represents the Fitness according to the size of the population. It is noted that the Fitness varies inversely as a function of the size of the population, as the figure shows; in this case we can see Fitness fluctuations for small number of population size, then the reduction of Fitness is obvious as the size of the population increases until a certain value of the population size where the Fitness remains steady when the population size increases.

Figure 5 shows the variations of the fitness according to the number of iterations. From this curve, we can see that fitness varies enormously with number of iterations. For variable iteration count values from 30 to 4000 iterations, Fitness overall trend is downward, fallen to about 0.4439 µm. We notice in this case how the number of iteration is significantly effects fitness more than the size of population does. Figure 6 shows the variations of the fitness according to the voltage intervals of the actuators. This histogram indicates that the best range (interval) of the current is variable from [$-1e^{-7}$ to $+1e^{-7}$] to obtain the best Fitness varies less than 0.61 µm. To conclude, the best configurations for the GA parameters that lead to the best wave-front corrections are those who correspond to population size ≥ 2000, iteration count ≥ 2500, and a voltage interval ($-1e^{-7}$ … $1e^{-7}$).

Table 3. Gentic algorithm parameters

	Value	Description
Min-coef	$-1e^{-7}$	Minimum value of voltage to be applied on DM actuators
Max-coef	$+1e^{-7}$	Maximum value of voltage to be applied on DM actuators
popSize	2500	Population size (Chromosomes number)
Chrom Size	80	Chromosome size (number of genes/actuators)
Iterations Count	≥3000	Genetic loops count
Cross Rate	60%	Crossover rate
Cross Points Count	40	Crossover points count
mutRate	70%	Mutation rate

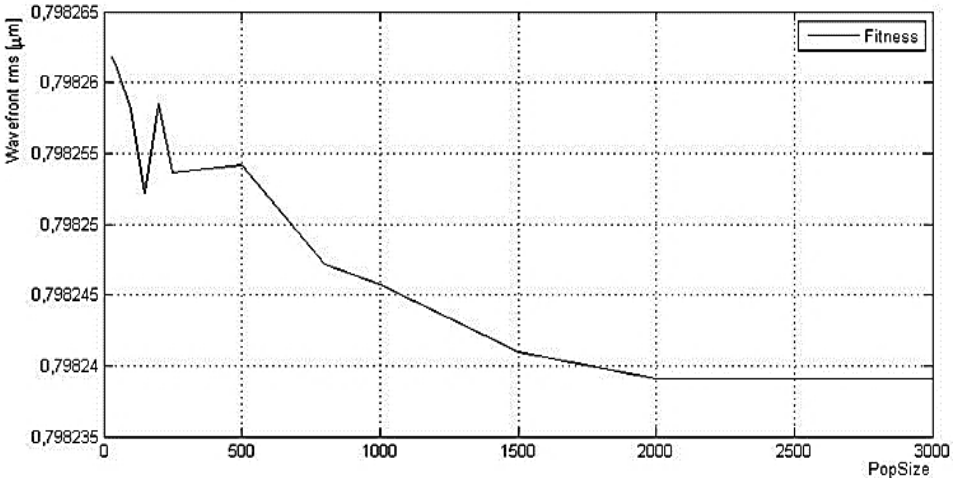

Figure 4. Wave-front correction as function of popsize

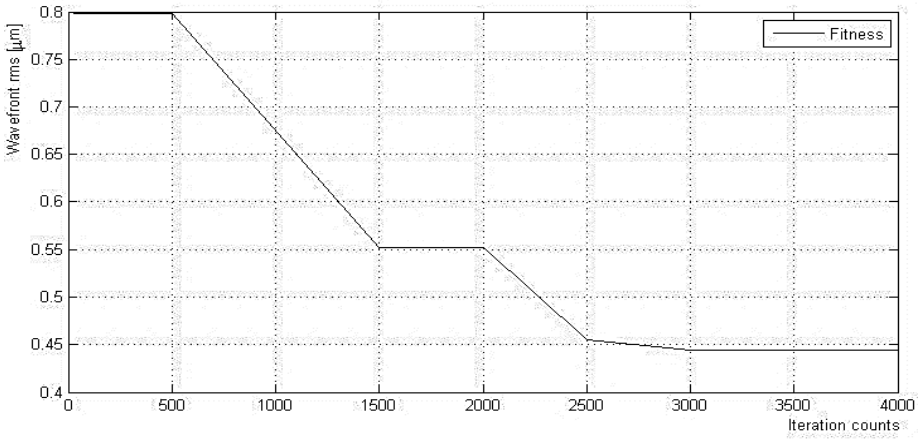

Figure 5. Wave-front correction as a function of iteration counts

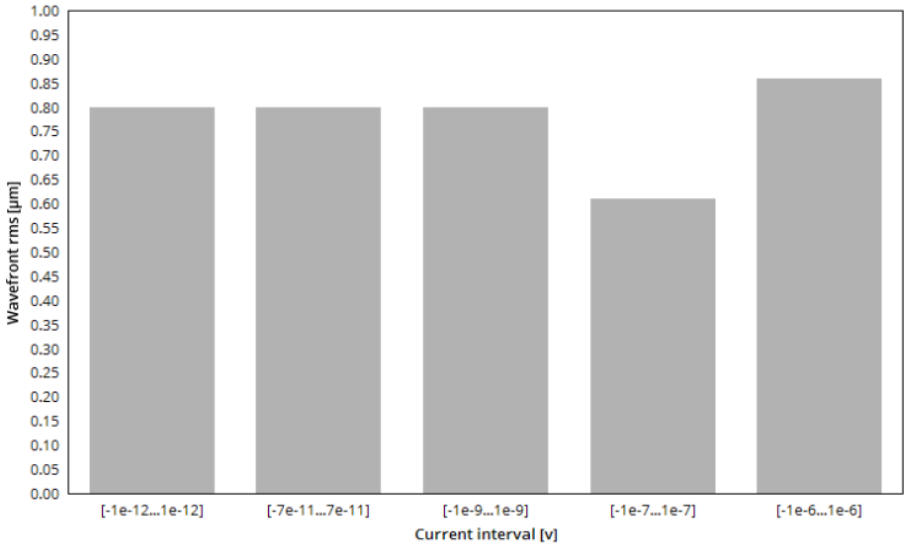

Figure 6. Histograms of wave-front corrections as a function of the actuator voltage intervals

4.3. Comparison between OOMAO and hybrid algorithm

We propose a hybrid solution (AO and GA). When the initial population of our GA is not totally random, we took some real solutions from the default OOMAO closed loop (50% and the rest of individuals are random), then we compare the results. Figure 7 represents results obtained from the comparison between the OOMAO which proposed in [26, 28] and our hybrid solution. It can clearly be seen that there has been a sharp decrease in both graphs between 0 and 200 iteration because 50% of suggested solutions are random. After 300, hybrid solution has only shown a slight growth. This is because algorithm excludes the wrong solutions and start keeping only the correct ones. After 200, the graph has a horizontal pitch. Between (2500-3000), there is a stability in hybrid solution graph which continues to drop making a better performance after 3000 iteration.

Overall, the graph illustrates the comparison between two solutions. Firstly, we notice that the values of hybrid solution is bigger than OA solution. That's because the number of iterations is small (less than 200) which leads to very weak result. Then, the number of iterations grows up making a better results because our GA is getting optimized by the time.

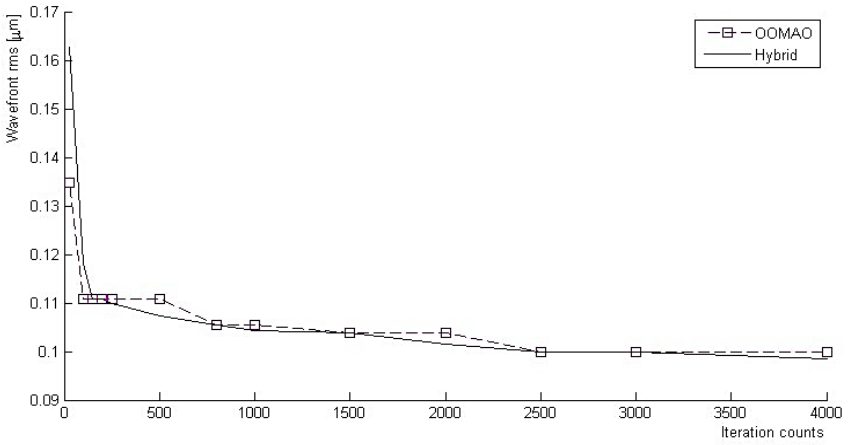

Figure 7. Comparison between OOMAO solution and the proposed hybrid solution

5. CONCLUSION

The genetic algorithm was applied in adaptive optical system to correct wave-front sensor in a disturbed atmosphere. Based on the OOMAO, we simulate the performance of an adaptive optical system with telescope (resolution 54, diameter 8m) and deformable mirror containing 92 actuators. We used the best parameters of the previous simulation (popSize 2500, Iterations count > 3000, min-volt $-1e^{-7}$, max-volt $+1e^{-7}$) to create hybrid solution (AO and GA). By comparing the obtained results, it was found that using this hybrid solution leads to better enhancement of AO performance than those produced by applying the OOMAO with the difference of 0.0279µm. We intend in future works to reduce the response time of the GA and develop more optimization algorithms particularly those related to the improvement of the wave-front sensor like: simulated annealing (SA), algorithm of pattern extraction (Alopex) and stochastic parallel gradient descent (SPGD).

REFERENCES

[1] Zhu X., Kahn J. M., "Free-space optical communication through atmospheric turbulence channels," *IEEE Transactions on Communications*, vol. 50, no. 8, pp. 1293-1300, August 2002.
[2] Ippolito L. J., "Radiowave propagation in satellite communications," *Springer Science & Business Media*, 2012.
[3] Arimoto Y., Hayano Y., Klaus W., "High-speed optical feeder-link system using adaptive optics," *Proceedings of SPIE - The International Society for Optical Engineering*, January 1997.
[4] Siles G. A., Riera J. M., Garcia-del-Pino P., "Atmospheric attenuation in wireless communication systems at millimeter and THz frequencies [Wireless Corner]," *IEEE Antennas and Propagation Magazine*, vol. 57, no. 1, pp. 48-61, February 2015.
[5] Barchers J. D., Fried D. L., "Optimal control of laser beams for propagation through a turbulent medium," *Journal of the Optical Society of America A (OSA)*, vol. 19, no. 9, pp. 1779-1793, 2002.

[6] Abozeed M. I., Alhilali M., Yin L. H., Din J., "Rain attenuation statistics for mobile satellite communications estimated from radar measurements in Malaysia," *TELKOMNIKA Telecommunication Computing Electronics and Control*, vol. 17, no. 3, pp. 1110-1117, June 2019.
[7] Alhilali M., Lam H., Din J., "Comparison of Raindrop Size Distribution Characteristics across the Southeast Asia Region," *TELKOMNIKA Telecommunication Computing Electronics and Control,* vol. 16, no. 6, pp. 2522-2527, December 2018.
[8] Badron K., Ismail A. F., Din J., Tharek A. R., "Rain induced attenuation studies for V-band satellite communication in tropical region*," Journal of Atmospheric and Solar-Terrestrial Physics*, vol. 73, no. 5-6, pp. 601-610, April 2011.
[9] Yang H., Li X., "Comparison of several stochastic parallel optimization algorithms for adaptive optics system without a wavefront sensor," *Optics & Laser Technology*, vol. 43, no. 3, pp. 630-635, April 2011.
[10] Chen E., Cheng H., An Y., Li X., "The Improvement of SPGD Algorithm Convergence in Satellite-to-Ground Laser Communication Links," *Procedia Engineering*, vol. 29, pp. 409-414, 2012.
[11] Avanaki M. R., Hojjatoleslami S., Sarmadi H., Ebrahimpour R., Podoleanu A. G., eds., "Genetic algorithm for optimization of optical systems," *2010 18th Iranian Conference on Electrical Engineering*, pp. 172-176, 2010.
[12] Jackson J. D., "Classical electrodynamics john wiley & sons," *Inc, New York*, pp. 832, 1999.
[13] Yu P., Glover I. A., Watson P., Davies O., Ventouras S., Wrench C., "Review and comparison of tropospheric scintillation prediction models for satellite communications," *International Journal of Satellite Communications And Networking*, vol. 24, no. 4, May 2006.
[14] Voyez J., "Mesures optiques de profils de turbulence atmosphérique pour les futurs systèmes d'optique adaptative," PhD Thesis, *Université Nice Sophia Antipolis*, 2013.
[15] Kolmogorov A. N., "The local structure of turbulence in incompressible viscous fluid for very large Reynolds numbers," *Proceedings of the Royal Society of London Series A: Mathematical and Physical Sciences*, vol. 434, no. 1890, pp. 9-13, July 1991.
[16] Brussard G. and Watson P. A., "Atmospheric modelling and millimetre wave propagation," *Springer Netherlands*, 1994.
[17] Cha J-W., Ballesta J., So P. T., "Shack-Hartmann wavefront-sensor-based adaptive optics system for multiphoton microscopy," *Journal of biomedical optics,* vol. 15, no. 4, July 2010.
[18] Rousset G., "Wave-front sensors," *Adaptive optics in astronomy*, 1999.
[19] Poyneer L. A., "Scene-based Shack-Hartmann wave-front sensing: analysis and simulation," *Applied Optics*, vol. 42, no. 29, pp. 5807-5815, 2003.
[20] Rais M., Morel J-M., Thiebaut C., Delvit J-M., Facciolo G., "Improving wavefront sensing with a Shack-Hartmann device," *Applied Optics*, vol. 55, no. 28, pp. 7836-7846, 2016.
[21] Weyrauch T., Vorontsov M. A., Bifano T. G., Hammer J. A., Cohen M., Cauwenberghs G., "Microscale adaptive optics: wave-front control with a μ-mirror array and a VLSI stochastic gradient descent controller," *Applied Optics*, vol. 40, no. 24, pp. 4243-4253, 2001.
[22] Grefenstette J. J., "Genetic algorithms and their applications," *proceedings of the second international conference on genetic algorithms*: Psychology Press, July 1987.
[23] Chambers L. D., "The practical handbook of genetic algorithms," applications: *Chapman and Hall/CRC*, pp. 544, December 2000.
[24] Nosato H., Itatani T., Murakawa M., Higuchi T., Noguchi H., "Automatic wave-front correction of a femtosecond laser using genetic algorithm," *2004 IEEE International Conference on Systems, Man and Cybernetics (IEEE Cat. No.04CH37583)*, The Hague, vol. 4, pp. 3675-3679, 2004.
[25] Yang P., Hu S., Chen S., Yang W., Xu B., Jiang W., "Research on the phase aberration correction with a deformable mirror controlled by a genetic algorithm," *Journal of Physics: Conference Series*, vol. 48, no. 1, pp. 1017-1024, October 2006.
[26] Conan R., Correia C., "Object-oriented Matlab adaptive optics toolbox," in *Proceedings of SPIE-The International Society for Optical Engineering,* pp. 9148-91486C, August 2014.
[27] Chulani H. M., Rodríguez-Ramos J. M., "Preliminary performance results of the weighted Fourier phase slope centroiding method for Shack–Hartmann wavefront sensors obtained with the OOMAO simulator," *Conference: Adaptive Optics for Extremely Large Telescopes V (AO4ELT5),* June 2017.
[28] Github E., "Ethereum rconan/OOMAO. Object-Oriented, Matlab & Adaptive Optics," 2018. [Online]. Available: https://github.com/rconan/OOMAO. 2018